Bmi1 regulates neural differentiation of mesenchymal stem cells through the Wnt3a-RhoA signaling pathway to repair ischemic brain injury in rats

KUNLING CHEN, HONGJIE ZHOU, JIE ZHANG, YIWEI ZHANG, XIAOBING DOU, QIN YU and LIPING ZHOU

School of Life Science, Zhejiang Chinese Medical University, Hangzhou, Zhejiang 310053, P.R. China

Received January 30, 2025; Accepted June 19, 2025

DOI: 10.3892/ijmm.2025.5596

Abstract. Ischemic brain injury (IBI) is characterized by high morbidity, disability and mortality rates; however, it lacks effective clinical treatments. Mesenchymal stem cells (MSCs), as pluripotent stem cells with self-renewal capacity and multilineage differentiation potential, have emerged as a promising therapeutic strategy for neurological disorders. In the present study, *in vitro* experiments were performed using the Wnt signaling agonist Wnt3a and the B lymphoma Mo-MLV insertion region 1 homolog (Bmi1) small molecule inhibitor PTC209 to treat MSCs, and the roles and regulatory mechanisms of the Bmi1 and Wnt3a-RhoA signaling pathways on the neural differentiation of MSCs were explored by MTT assay, immunofluorescence analysis and western blotting. *In vivo* experiments were also performed by establishing a rat model of middle cerebral artery occlusion (MCAO), transplanting different MSCs into the rat brain tissues after *in vitro* labeling, and comparing ischemic brain damage in each group of rats by Neurological Severity Score scoring, grasp assay, triphenyltetrazolium chloride staining, hematoxylin and eosin staining, and assessing neurological recovery via immunofluorescence and western blot analysis. The *in vivo* study aimed to assess the roles of the Bmi1 and Wnt3a-RhoA signaling pathways in brain injury repair in MCAO rats and the mechanism. Specifically, recombinant Wnt3a cytokine was administered to upregulate the Wnt3a-RhoA pathway, whereas the small-molecule inhibitor PTC209 was utilized to suppress Bmi1 expression. The findings suggested that Bmi1 modulates the neural differentiation of MSCs through its regulatory effects on Wnt3a and RhoA expression, thereby influencing the reparative potential of MSCs in ischemic brain tissue. These findings highlight the therapeutic relevance of targeting Wnt3a-RhoA activation and Bmi1 inhibition in MSC-based interventions for IBI.

Correspondence to: Professor Qin Yu or Dr Liping Zhou, School of Life Science, Zhejiang Chinese Medical University, 548 Binwen Road, Hangzhou, Zhejiang 310053, P.R. China
E-mail: qinyu3587@126.com
E-mail: lipingzhou@zcmu.edu.cn

Abbreviations: MSC, mesenchymal stem cell; Bmi1, B lymphoma Mo-MLV insertion region 1 homolog; IBI, ischemic brain injury; BME, β-mercaptoethanol; NSC, neural stem cell; PCP, planar cell polarity; SDF-1α, stromal cell-derived factor-1α; FBS, fetal bovine serum; DMSO, dimethyl sulfoxide; TTC, triphenyltetrazolium chloride; NSS, Neurological Severity Score; MCAO, middle cerebral artery occlusion; H&E, hematoxylin and eosin

Key words: MSCs, Bmi1, IBI, Wnt3a-RhoA signaling pathway

Introduction

Ischemic brain injury (IBI) is a leading cause of disability and death worldwide. In China, it has been categorized as one of the important causes of disease-related deaths (1). The condition is primarily caused by the narrowing or blockage of blood vessels, which leads to insufficient blood and oxygen supply to the brain tissue; this, in turn, causes necrosis or apoptosis of neurons in the brain tissue, resulting in irreversible neurological damage. A number of patients who survive may experience long-term neurological sequelae, such as cerebral palsy, paraplegia and other lifelong disabilities. Currently, clinical treatment for IBI entails symptomatic support, cerebrovascular circulation improvement, neuroprotective medication or interventional therapy, such as endovascular stenting and percutaneous transluminal angioplasty. However, the administration of therapy is impeded by the blood-brain barrier, and recurrence of the intervention is possible, with incomplete repair of the infarcted area (2,3). Mesenchymal stem cells (MSCs) are adult stem cells with the capacity for self-renewal and multidirectional differentiation, and under certain conditions they can be differentiated into various neural cells across the embryonic layer (4,5). Research has shown that MSCs possess the ability to repair tissue damage when locally transplanted, intravenously or intra-arterially administered after an injury (6,7). Furthermore, MSCs have been shown to possess the capacity to survive, migrate, integrate and differentiate into neuronal cells within living organisms. The utilization of MSCs to address neurological disorders through the replacement of defective or damaged neural tissues represents a promising therapeutic strategy that circumvents various challenges. These challenges include the scarcity of adult neural stem cells (NSCs), the difficulties involved in their isolation and culture, and the ethical and immunological problems that are associated with them (8).

Notably, obstacles to the clinical application of MSCs persist. MSCs necessitate hundreds of millions of cells *in vitro*, and although MSCs can be harvested from a range of organs, the number of isolated cells is inadequate (9) and long-term expansion *in vitro* is required to obtain enough stem cells. However, as the number of passages increase, MSCs display senescence characteristics, including changes in cell morphology, reduced proliferation and diminished directed differentiation ability (10-12). The loss of stemness in MSCs during *in vitro* culture, their low survival rates following transplantation, and compromised self-renewal and differentiation capacities collectively pose major obstacles to the clinical translation of MSC-based therapies. Therefore, enhancing the regulatory mechanisms that sustain MSC proliferation, migration and differentiation *in vivo* is critical for optimizing MSC transplantation efficacy in treating neurological disorders and promoting the recovery of neurological function.

The neural differentiation of adult stem cells is regulated by various factors, with epigenetic mechanisms serving a crucial role in precisely controlling gene expression (13). Polycomb family proteins are notable epigenetic regulators of adult stem cells, comprising mainly of two protein complexes: PRC1 and PRC2. B lymphoma Mo-MLV insertion region 1 homolog (Bmi1), discovered in 1991, is localized on human chromosome 10p12.2 locus, and consists of nine exons and nine introns, mainly encoding poly sparse histones (components of PRC1-like complexes) (14). PRC1 complexes containing Bmi1 proteins can act through chromatin remodeling and histone modifications to cause epigenetic alterations (15). Numerous studies have confirmed that Bmi1 is crucial for neurogenesis *in vivo* (16). Notably, knocking down the Bmi1 gene has been shown to disrupt the stable development of NSCs, hamper NSC proliferation and leads to an increase in glial cells (17). Previous studies (18,19) demonstrated that, through Bmi1 knockdown experiments, Bmi1 serves a crucial role in the proliferation and survival of cortical bone-derived stem cells.

Previous studies have demonstrated that Bmi1 can regulate the expansion capacity of mammary epithelial cells and fibroblasts *in vitro* and *in vivo* through the Wnt signaling pathway (20). The Wnt signaling pathway is one of the major signaling pathways that regulate cell proliferation and differentiation, including the classical Wnt/β-catenin pathway and the non-classical Wnt pathway. Our prior research has shown that the Wnt/β-catenin signaling pathway notably impacts the neural differentiation process of MSCs (21,22). The non-classical Wnt pathway is less explored and more complex than the classical Wnt/β-catenin pathway. The planar cell polarity (PCP) signaling pathway is a specific type of non-classical Wnt pathway that controls cell motility and cellular differentiation; this pathway triggers signaling cascades via cytoplasmic cytoskeletal proteins, RhoA, Rac-activated c-Jun amino-terminal kinases and Rho-associated kinases (23). Wnt3a is the primary ligand responsible for Wnt signaling pathways, as research has indicated that when Wnt3a binds to the cell membrane receptor, it extracellularly activates both the Wnt/β-catenin signaling pathway and the nonclassical Wnt signaling pathway (24). RhoA is present in the cell as a bound form in the signaling pathway and serves as a downstream element of the PCP pathway. RhoA, along with its regulatory proteins, has crucial roles in neural differentiation (25). Nonetheless, it remains unclear whether Bmi1 has the ability to regulate neural differentiation in MSCs through the Wnt3a-RhoA pathway.

The present study therefore investigated the role of Bmi1 in regulating the Wnt3a-RhoA signaling pathway and promoting neural differentiation of MSCs *in vitro*. In addition, a middle cerebral artery occlusion (MCAO) model was established *in vivo* to evaluate the therapeutic potential of MSC transplantation in IBI. To assess this, recombinant Wnt3a cytokine was administered to upregulate the Wnt3a-RhoA pathway, whereas the small-molecule inhibitor PTC209 was utilized to suppress Bmi1 expression.

Materials and methods

Animals. In the present study, male Sprague-Dawley (SD) rats (weight, 80-120 g; age, 2-4 weeks) were used for MSC isolation and culture. One rat was required for each T25 cell culture flask of primary MSCs collected, and 33 male SD rats were used for MSC isolation. The MCAO model was established using 45 male SD rats (weight, 260-300 g; age, 6-8 weeks). All rats were provided by Zhejiang Chinese Medical University Animal Center (Laboratory Animal Certificate: SCXK 2018-0006; Hangzhou, China). The rats were maintained at a temperature of 20±2˚C, a humidity of 55±5%, under a 12-h light/dark cycle, and were given free access to food and water. All animal experiments were approved by the Animal Ethical and Welfare Committee of Zhejiang Chinese Medical University (approval no. 20210524-05, review no. IACUC-202108-05). All SD rats in all experiments were euthanized by intravenous injection of an overdose of pentobarbital (100 mg/kg), which was confirmed by observing their vital signs 10 min after administration.

Chemicals. Wnt3a recombinant cytokine (cat. no. 96-315-20-10) was purchased from PeproTech; Thermo Fisher Scientific, Inc. and the small molecule inhibitor PTC209 (cat. n. S7372) was purchased from Selleck Chemicals. Before use, Wnt3a powder was dissolved in sterile water, and PTC209 powder was dissolved in dimethyl sulfoxide (DMSO). A quantity of 10 mg PTC209 powder was dissolved in 1.14 ml DMSO to create a 2 mmol/l master mix.

Isolation and culture of rat MSCs. MSCs were obtained from rat bone marrow by flushing the contents of the tibia and femur with phosphate-buffered saline (PBS) in a sterile environment, and were then transferred to a centrifuge tube to be centrifuged at 10,000 x g for 5 min at room temperature. After centrifugation, the supernatant was discarded, and the cells were resuspended in MSC medium prepared with DMEM/F-12 (cat. no. TBD10565; Tianjin Haoyang Biological Products Technology Co., Ltd.) containing 10% fetal bovine serum (FBS; cat. no. 10091-148; Gibco; Thermo Fisher Scientific, Inc.) and 1% penicillin-streptomycin solution, and were inoculated in T25 cell culture flasks at a temperature of 37˚C in a 5% CO_2 incubator. Cell morphology was observed under an inverted fluorescence microscope (ECLIPSE TE2000-U; Nikon Corporation).

Cell proliferation assay. MSCs were cultured in 96-well plates with varying concentrations of recombinant cytokine Wnt3a (0, 10, 50 and 100 ng/ml) and a small molecule inhibitor PTC209 (0, 1, 2.5, 5 and 10 μmol/l). Each group was subjected to a 24-h stimulation period within a 37˚C incubator, comprising five replicate wells at varying concentrations. Subsequently, the cells were exposed to 5 mg/ml MTT for 4 h, the blue-violet formazan crystals were dissolved in DMSO and the absorbance was measured at 450 nm using an enzyme-linked instrument. The MTT kit was purchased from Abcam (cat. no. ab211091).

In vitro induction of neural differentiation in MSCs. The 3rd-5th generation MSCs in logarithmic growth phase were collected and inoculated in two 6-well plates at a cell density of $1x10^5$ cells/ml. The cells were randomly divided into four groups (n=3 wells each): Normal control (NC) group, β-mercaptoethanol (BME) group, Wnt3a group and PTC209 group. The NC group comprised normal cultured cells without induction of neural differentiation; the BME group was pre-induced with neural differentiation pre-induction medium for 24 h, followed by induction with neural differentiation medium for 3-6 h. The Wnt3a group and the PTC209 group were treated with neural differentiation medium containing 10 ng/ml Wnt3a and 1 μmol/ml PTC209, respectively, and the incubation steps were the same as that of the BME group. The neural differentiation pre-induction medium consisted of DMEM/F-12 supplemented with 20% FBS, 1 mmol/l BME and 1% penicillin-streptomycin solution. The neural differentiation induction medium was prepared by adding 5 mmol/l BME and 1% penicillin-streptomycin solution to DMEM/F-12.

Immunofluorescence staining of MSCs. The culture medium in the cell plates was aspirated and discarded, and the cells were washed with PBS and fixed with 4% paraformaldehyde at room temperature for 10 min. The cells were washed again with PBS and cell membranes were ruptured with a permeabilizing solution of 0.5% TritonX-100 (cat. no. V900502; MilliporeSigma) at room temperature for 10 min. After further washing with PBS, the cells were blocked in PBS containing 2% BSA (cat. no. 9048-46-8; Shanghai Macklin Biochemical Co., Ltd.) and 0.1% Tween-20 (cat. no. 9005-64-5; Shanghai Macklin Biochemical Co., Ltd.) for 1 h at room temperature. The appropriate primary antibody dilutions were then added and incubated overnight at 4˚C. Subsequently, the primary antibody was removed, the cells were washed three times with PBS (8 min each) and the corresponding secondary antibody dilution was added and incubated in the dark for 1 h at room temperature. Both primary and secondary antibodies were prepared at a ratio of 1:200. Finally, DAPI staining solution was added in the dark, and the cells were observed and images were captured under an inverted phase contrast fluorescence microscope to detect neuronal cell markers. The intermediate filament protein nestin is a common specific marker for NSCs, which is mainly expressed in the cytoplasm; NeuN is a neuron-specific nuclear protein; Olig2 is an oligodendrocyte-specific marker; glial fibrillary acidic protein (GFAP) is primarily found in astrocytes within the central nervous system and is a commonly used cellular marker. The primary antibodies anti-GFAP (cat. no. ab7260), anti-NeuN (cat. no. ab177487), anti-nestin (cat. no. ab254048) and anti-Olig2 (cat. no. ab254043), and the Goat Anti-Rabbit IgG H&L (Alexa Fluor® 488) secondary antibody (cat. no. ab150077) were obtained from Abcam. The antibodies were diluted with 5% BSA solution according to the instructions.

Modeling of rat MCAO. The rats were deprived of food for 12 h prior to surgery and administered an intraperitoneal injection of 3% sodium pentobarbital (45 mg/kg, provided by the Animal Experiment Center of Zhejiang University of Traditional Chinese Medicine) for anesthesia. The rat MCAO model was created using the modified Zea Longa wire bolus method. The rats were immobilized in the supine position, and an incision was made in the midline of the neck. The right common carotid artery (CCA), external carotid artery (ECA) and internal carotid artery (ICA) were sequentially isolated, and threads (4-0 sutures) were placed distal and proximal to the CCA and at the ECA. The ICA was temporarily clamped with a microarterial clip, and then the CCA and ECA were ligated proximally. Subsequently, a small opening was cut with scissors 4 mm from the bifurcation of the CCA, the prepared suture was inserted into the ICA, and the suture was tied securely with a thin wire wrapped around the distal end of the CCA when the marked point on the suture reached the bifurcation. The wound was covered with a saline-soaked cotton ball to keep it moist, and after 1.5 h of embolization, the suture was removed, the vessels were ligated, and the wound was sutured and disinfected. Rats were scored according to the Longa 5-point scale (26) on day 3 after modeling, and modeling was considered successful in rats with ≥1 point.

CM-Dil labeling of MSCs. The 3rd-5th generation MSCs in logarithmic growth phase were collected, and after discarding the original medium, they were rinsed twice with PBS. Staining solution was prepared by adding the labeling solution to the medium in a ratio of 1 ml MSC medium: 1 μl CM-Dil labeling solution (cat. no. C7000; Invitrogen; Thermo Fisher Scientific, Inc.). The cells were incubated in a CO_2 incubator at 37˚C for 10-20 min after the addition of the staining solution. At the end of the incubation, the cells were rinsed twice with PBS and then incubated again at 4˚C for 15 min to avoid staining of the nuclei. The MSCs that had been labeled with CM-Dil were cultured for a further 24 h, and were then observed and images were captured under an inverted fluorescence microscope, which was used to detect the survival of MSCs in brain tissues after subsequent cell transplantation.

Brain stereotactic transplantation of MSCs and animal grouping. On day 3 after modeling, the rats were anesthetized by inhalation of 4% isoflurane through a mask, fixed into a brain stereotaxic apparatus, sterilized and a 10 μl suspension of MSCs (10^7 cells/ml) was injected into the injection sites of the hippocampus at a rate of 1 μl/min. The rats were observed for infection and mortality.

A total of 45 SD rats were randomly assigned to five groups: Sham, MCAO, MSCs, Wnt3a-MSCs and PTC209-MSCs (n=9 rats/group). The Sham and MCAO groups were transplanted with 10 μl PBS on the postoperative day 3, the MSCs group was transplanted with MSCs on postoperative day 3, the Wnt3a-MSCs group was transplanted

with 10 ng/ml Wnt3a-treated MSCs on day 3 after modeling, and the PTC209-MSCs group was transplanted with 1 μmol/l PTC209-treated MSCs on postoperative day 3. MSCs in each group were pretreated for 48 h.

Neurological function tests. The neurological injury severity in rats was assessed using the Neurological Severity Score (NSS) on days 1, 3, 5 and 7 after MSC transplantation. The rat tail was lifted 30 cm off the ground and the forelimbs were observed. Rats with both forelimbs symmetrically extended to the ground, with the left shoulder internally rotated and the left forelimb internally retracted were considered normal and rated 4 points, otherwise they were rated 0 points. In addition, the rat was placed on a smooth floor and resistance to movement was examined by pushing the left (or right) shoulder to the opposite side, respectively. Rats with resistance that was clearly symmetrical on both sides were considered normal (0 points); when the resistance was decreased, this was rated 1-3 points according to the degree of decrease. Furthermore, the two forelimbs of the rats were placed on a metal net and the tension of the two forelimbs was observed. When the tension of the two forelimbs was obviously symmetrical, this was considered normal (0 points); when the muscle tension of the left forelimb decreased, this was rated 1-3 points according to the degree of decrease. Based on the aforementioned scores out of 10, the higher the score, the more severe the behavioral disorder.

Grip assays were also performed on days 1, 3, 5 and 7 after transplantation of MSCs. In order to measure grip force, the grip force measuring instrument was placed on a horizontal table and levelled so that the grip force plate was in a horizontal direction. The rat was then gently placed on the grip plate and the tail was pulled back horizontally to record the maximum grip force of the rat.

Triphenyltetrazolium chloride (TTC) staining. On day 7 after MSC transplantation, intact brain tissues were obtained from three randomly selected rats in each group after euthanasia.; the animals were euthanized as aforementioned. These tissues were placed in a pre-cooled tank (4˚C), rapidly frozen at -20˚C for 20 min, and 2-mm coronal sections were cut and placed in 2% TTC dye at 37˚C away from light for 15 min. After staining, images were captured, and were processed using the Image-Pro Plus 6.0 image analysis system software (Media Cybernetics, Inc.) to calculate the infarction rate of the rat brain tissue.

Hematoxylin and eosin (H&E) staining. On day 14 after the transplantation of MSCs, three rats in each group were randomly selected for the removal of intact brain tissues, which were subjected to H&E staining to observe the pathological changes in the CA1 area of the hippocampus in each group. The animals were euthanized as aforementioned. Brain tissues were fixed with 4% paraformaldehyde at 4˚C for 24 h, embedded in paraffin and were cut into 5-10 μm slices on a sectioning machine at 4˚C. Tissue sections were deparaffinized with xylene two times (10 min each), hydrated with a descending series of ethanol concentrations, washed with water and distilled water, and stained with hematoxylin for 5 min. Subsequently, the sections were washed with water, incubated with 1% hydrochloric acid and 70% ethanol for 3 sec, washed with water for 10 min and stained with 1% eosin for 1 min. Finally, the sections were washed with water, dehydrated in an ascending series of ethanol concentrations, permeabilized twice with xylene (1 min each) and sealed with neutral gum. Finally, the sections were observed and images were captured under a light microscope.

Immunofluorescence staining. On day 14 after transplantation of MSCs, three brain tissue sections were randomly collected from each group. Rat brain tissues were fixed in 4% paraformaldehyde for 8 h at room temperature., dehydrated in 30% sucrose solution, and embedded in OCT embedding agent, before being frozen at -80˚C. Subsequently, the tissues were sectioned into 5-10 μm slices. Subsequently, 3% H_2O_2 was added dropwise to the sections and incubated at 37˚C for 10 min to block endogenous peroxidase, after which, the sections were rinsed with distilled water three times (5 min each). The sections were then placed in boiling sodium citrate buffer solution and reacted at 92-98˚C for 20 min for antigen retrieval. After cooling, the slices were washed three times with PBS solution (2 min each). Immunofluorescence was then performed as aforementioned for MSCs, using the same antibodies.

Western blotting. The MSCs of each group, as well as the ischemic penumbra tissues and hippocampal tissues on the damaged side of the rat brain of each group, were lysed with protein lysis solution (cat. no. 89900; Thermo Fisher Scientific, Inc.) on ice. The supernatant was collected after centrifugation at 10,000 x g for 15 min at 4˚C after lysis. Following the extraction of total proteins from the cells and tissues, the protein concentration was detected according to the instructions in the BCA kit (cat. no.AR0146; Boster Biological Technology). Depending on the molecular weight of the protein, a 10 or 12% separation gel was prepared, and 20 μg proteins underwent SDS-PAGE. Proteins were then transferred to polyvinylidene fluoride membranes, which were blocked with a ready-to-use 5% skimmed milk powder sealer. The membranes were then incubated at 4˚C overnight with the following primary antibodies: Anti-Bmi1 (cat. no. ab38295), anti-RhoA (cat. no. ab187027), anti-Wnt3a (cat. no. ab219412) (all from Abcam) and anti-β-actin (cat. no. BK7018; Bioker), anti-GFAP (cat. no. ab7260), anti-NeuN (cat. no. ab177487) and anti-nestin (cat. no. ab254048) (all from Abcam). Primary antibodies were diluted and prepared in 5% BSA solution at a ratio of 1:1,000 according to the antibody instructions. Subsequently, the membranes were incubated for 2 h at room temperature with a Goat Anti-Rabbit IgG H&L (Alexa Fluor® 488) secondary antibody (cat. no. ab150077; Abcam), which was diluted and prepared according to the antibody instructions. Images of membranes were captured using an ultrasensitive chemiluminescent substrate kit (cat. no. AR1111; Boster Biological Technology) utilizing a chemiluminescent imaging system (cat. no. 6000; Clinx Science Instruments Co., Ltd.) was used to capture images of the membranes, which were subsequently analyzed via ImageJ v1.8.0 analysis software (National Institutes of Health) for semi-quantification.

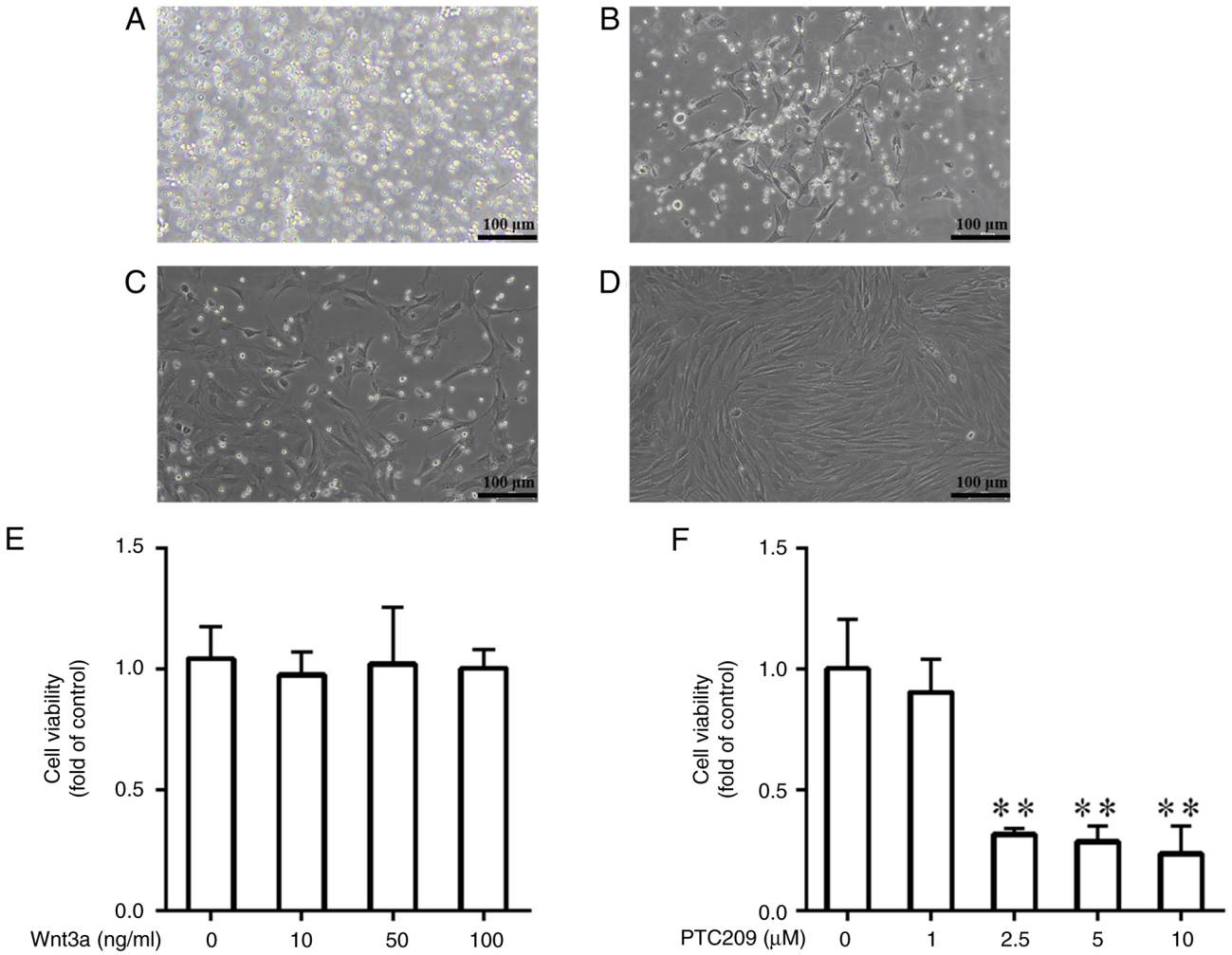

Figure 1. Effects of B lymphoma Mo-MLV insertion region 1 homolog and Wnt3a on the proliferation of MSCs. (A) Morphology of primary MSCs inoculated into culture flasks. Morphology of MSCs in primary culture for (B) 3 and (C) 7 days. (D) Morphological characterization of third-generation MSCs. Effects of different concentrations of (E) Wnt3a and (F) PTC209 on the proliferation of MSCs. **P<0.01 vs. 0 μM group. MSCs, mesenchymal stem cells.

Statistical analysis. All experiments were repeated more than three times. The experimental data were statistically analyzed using SPSS 25.0 (IBM Corp.). Experimental data are presented as the mean ± standard deviation and bar graphs were constructed using GraphPad Prism 9 (Dotmatics). A χ^2 test for variance was performed on the experimental data to assess distribution of data. One-way analysis of variance was used to compare the differences between groups and the data were analyzed by Tukey's post-hoc test for multiple comparisons between groups. The analysis of NSS scores was performed using the Kruskal-Wallis test followed by Dunn's post hoc test. P<0.05 was considered to indicate a statistically significant difference.

Results

MSC isolation culture and proliferative activity. Primary MSCs were cultured in T25 cell culture flasks and allowed to adhere to the wall and aggregate for 3 days. By day 7, the cells had formed colonies and were vigorously proliferating and dividing. Under a microscope, the cells were found to be either polygonal or irregularly shuttle-shaped (Fig. 1A-C). When the primary cultured MSCs reached 80-90% fusion, passaging culture was performed. Subsequently, MSCs experienced an increase in proliferative activity, as well as a continuous improvement in purity. Furthermore, their cell morphology gradually changed from an irregular polygonal shape to a shuttle or spindle shape (Fig. 1D). Different concentrations of Wnt3a (0, 10, 50 and 100 ng/ml) and Bmi1 small molecule inhibitor PTC209 (0, 1, 2.5, 5 and 10 μmol/l) were utilized to treat MSCs for 24 h, and the impact of both on cell viability was measured through MTT analysis. The results indicated that the viability of MSCs was normal in all groups of Wnt3a-treated cells, and there was no significant difference in the proliferative activity of MSCs between the different concentration groups, thus indicating that Wnt3a treatment did not affect the activity of MSCs (Fig. 1E). By contrast, in the cell groups treated with PTC209, that 1 μmol/l PTC209 had no significant effect on cell viability, whereas 2.5, 5 and 10 μmol/l PTC209 had a toxic effect on cells (Fig. 1F). Combining the findings of previous studies (27,28) and the present experimental results, 10 ng/ml Wnt3a and 1 μmol/l PTC209 were selected for subsequent experiments in the current study.

Wnt3a promotes and PTC209 inhibits differentiation of MSCs toward neurons. Compared with untreated MSCs, after 3 h of neural differentiation, the cytoplasm of MSCs contracted,

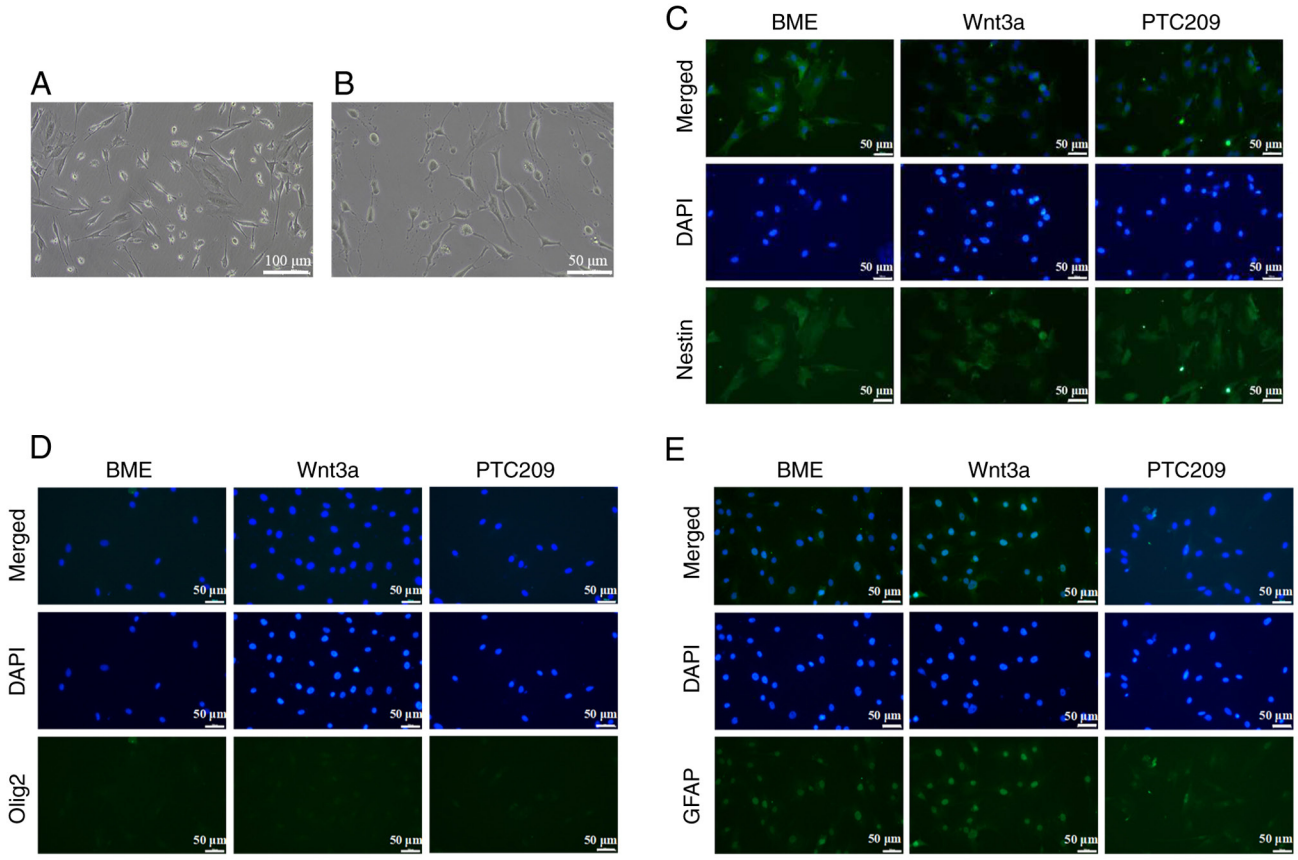

Figure 2. Role of Bmi1 in neural differentiation of MSCs. (A and B) Morphology of third-generation MSCs induced to neurally differentiate for 3 h; scale bars, (A) 100 μm and (B) 50 μm. (C) Effects of Wnt3a and Bmi1 on the expression of the neural stem cell marker Nestin. (D) Effects of Wnt3a and Bmi1 on the expression of Olig2. (E) Effects of Wnt3a and Bmi1 on the expression of GFAP. BME, β-mercaptoethanol; Bmi1, B lymphoma Mo-MLV insertion region 1 homolog; GFAP, glial fibrillary acidic protein; MSCs, mesenchymal stem cells.

longer synapses were formed, tiny branches appeared to converge into a meshwork, the cells grew well and a neuronal cell-like appearance was presented (Fig. 2A and B). MSCs induced by neural differentiation for 3 h could therefore be used for subsequent experiments. The BME, Wnt3a and PTC209 groups demonstrated specific green fluorescence of Nestin, indicating Nestin positive expression (Fig. 2C). In addition, the immunofluorescence results indicated the absence of marked green fluorescence in both the nucleus and cytoplasm following Olig2 staining; double-color staining of the nucleus and cytoplasm was not observed under a microscope, thus establishing that the expression of Olig2 was negative in all cell groups (Fig. 2D). Furthermore, after inducing neural differentiation of MSCs *in vitro*, the cytoplasm and nucleus emitted green fluorescence following GFAP staining; GFAP-positive cells could be clearly seen under the microscope in the BME and Wnt3a groups, whereas GFAP-positive cells were almost unobservable in the PTC209 group (Fig. 2E).

As determined by western blotting, the protein expression levels of Nestin were enhanced in the BME, Wnt3a and PTC209 groups compared with those in the NC group; however, no significant difference emerged between the three groups (Fig. 3). In addition, the protein levels of NeuN were significantly increased in the BME group compared with those in the NC group, and were significantly higher in the Wnt3a group compared with in the BME group. By contrast, NeuN protein expression levels were significantly lower in the PTC209 group compared with those in the BME group.

These findings indicated that BME stimulated MSCs to differentiate into NSCs *in vitro*, but not towards downstream oligodendrocyte lineage cells. Furthermore, Wnt3a treatment enhanced the differentiation of MSCs towards neurons, whereas PTC209 treatment impeded the differentiation of MSCs into astrocytes and neurons.

Bmi1 regulates the protein expression of Wnt3a and RhoA in vitro. The protein expression levels of Bmi1, Wnt3a and RhoA were significantly increased in the BME group compared with those in the NC group (Fig. 4). In comparison with the BME group, the protein expression levels of Wnt3a and RhoA were increased in the Wnt3a group; however, there was no significant difference in Bmi1 protein expression. By contrast, the protein expression levels of Bmi1, Wnt3a and RhoA were significantly decreased in the PTC209 group compared with those in the BME group. These findings indicated that Bmi1 may be implicated in the neural differentiation process of MSCs by controlling the expression of Wnt3a and RhoA.

Engraftment and survival of MSCs in ischemically injured brain tissue. In the present study, SD rats were subjected to the experiment shown in Fig. 5A. When cultured *in vitro* to the third generation, MSCs displayed spindle-shaped morphology with high homogeneity (Fig. 5B), and CM-Dil-labeled MSCs

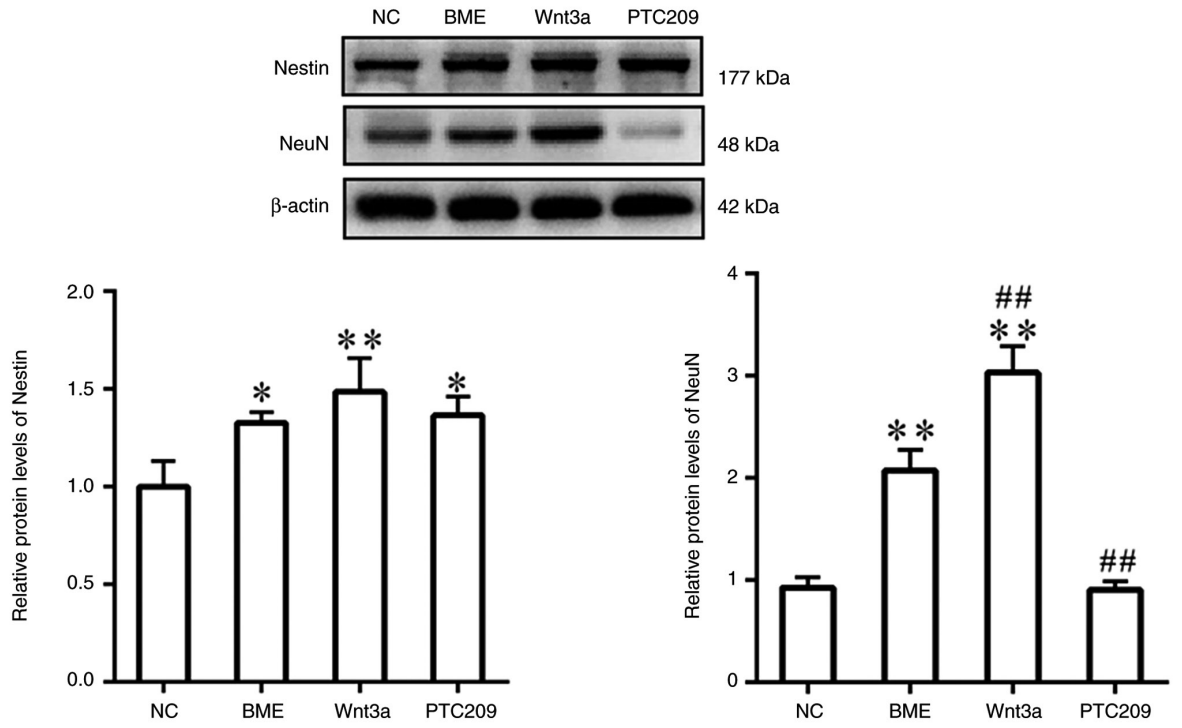

Figure 3. Effects of Wnt3a and B lymphoma Mo-MLV insertion region 1 homolog on neuronal marker expression. *P<0.05, **P<0.01 vs. NC; ##P<0.01 vs. BME. BME, β-mercaptoethanol; NC, normal control.

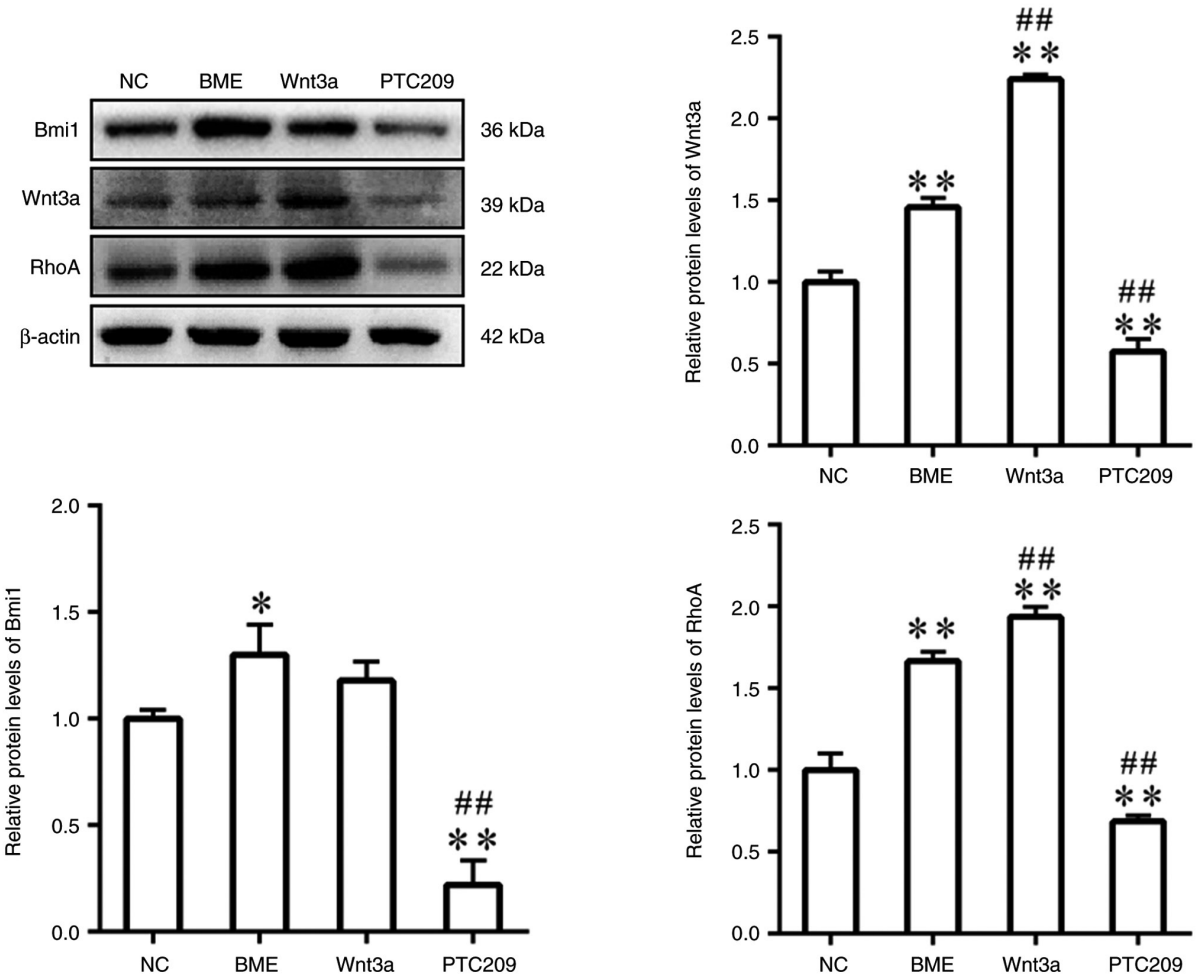

Figure 4. Expression of Bmi1 and Wnt3a-RhoA signaling pathway-related proteins in each group. *P<0.05, **P<0.01 vs. NC; ##P<0.01 vs. BME. BME, β-mercaptoethanol; Bmi1, B lymphoma Mo-MLV insertion region 1 homolog; NC, normal control.

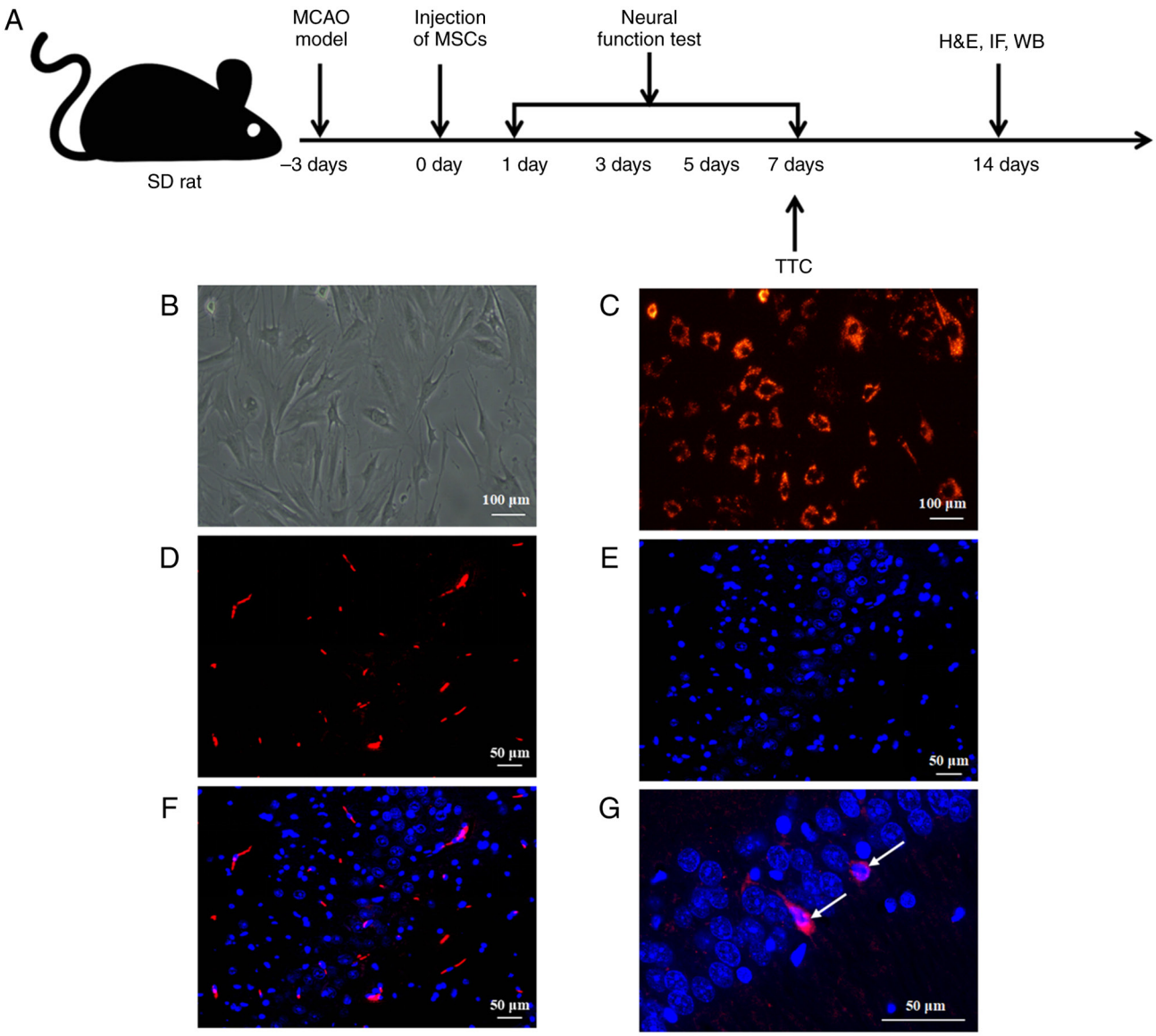

Figure 5. Detection of CM-Dil fluorescence labeling of MSCs *in vivo* and *in vitro*. (A) Experimental flowchart. (B) Morphology of third-generation MSCs. (C) CM-Dil *in vitro* labeling of MSCs. Results of (D) CM-Dil fluorescence detection and (E) DAPI staining in slices of the CA1 hippocampal region of brain tissue. (F) Results of co-localization of (D) and (E). (G) Results of co-localization of CM-Dil and DAPI staining in the CA1 hippocampal region. Arrows show MSCs transplanted into brain tissue. H&E, hematoxylin and eosin; IF, immunofluorescence; MCAO, middle cerebral artery occlusion; MSCs, mesenchymal stem cells; SD, Sprague-Dawley; TTC, triphenyltetrazolium chloride; WB, western blotting.

exhibited strong red fluorescence with an uncolored nucleus and high labeling efficiency (Fig. 5C). A total of 7 days after MSCs transplantation the rats were sacrificed and their brain tissues were analyzed using fluorescence detection. The transplanted cells were visibly labeled with red fluorescence after CM-Dil labeling (Fig. 5D), and blue cell fluorescence was observed following DAPI staining (Fig. 5E). The cells that displayed co-localization of red and blue fluorescence were considered MSCs that had been implanted in the brain tissue (Fig. 5F and G). These findings indicated that the MSCs were successfully transplanted into the brain tissues of rats that had IBI and were viable.

Bmi1 downregulation inhibits repair of IBI by MSC transplantation. The NSS scores demonstrated that rats in the Sham group obtained a score of 1 on days 1, 3, 5 and 7, and displayed no observable behavioral abnormalities (Fig. 6A). Conversely, rats in the MCAO group exhibited substantial behavioral deficits, including left shoulder internal rotation, decreased unilateral resistance to countermovement, and grip strength reduction on the left side due to IBI. There were no significant differences between the three groups receiving MSC transplantation on days 1, 3 and 5 when compared with the MCAO group; however, on day 7, rats in the MSC and Wnt3a-MSC groups had lower scores compared with in the MCAO group, whereas the PTC209-MSC group showed no significant change compared with the MCAO group. Furthermore, the results suggested that rats in the MCAO group had significantly weaker grasping strength than those in the Sham group on days 1, 3, 5 and 7 (Fig. 6B). On day 7, the MSCs group showed an improvement in grasping strength compared with the MCAO group. Furthermore, the Wnt3a-MSCs group exhibited

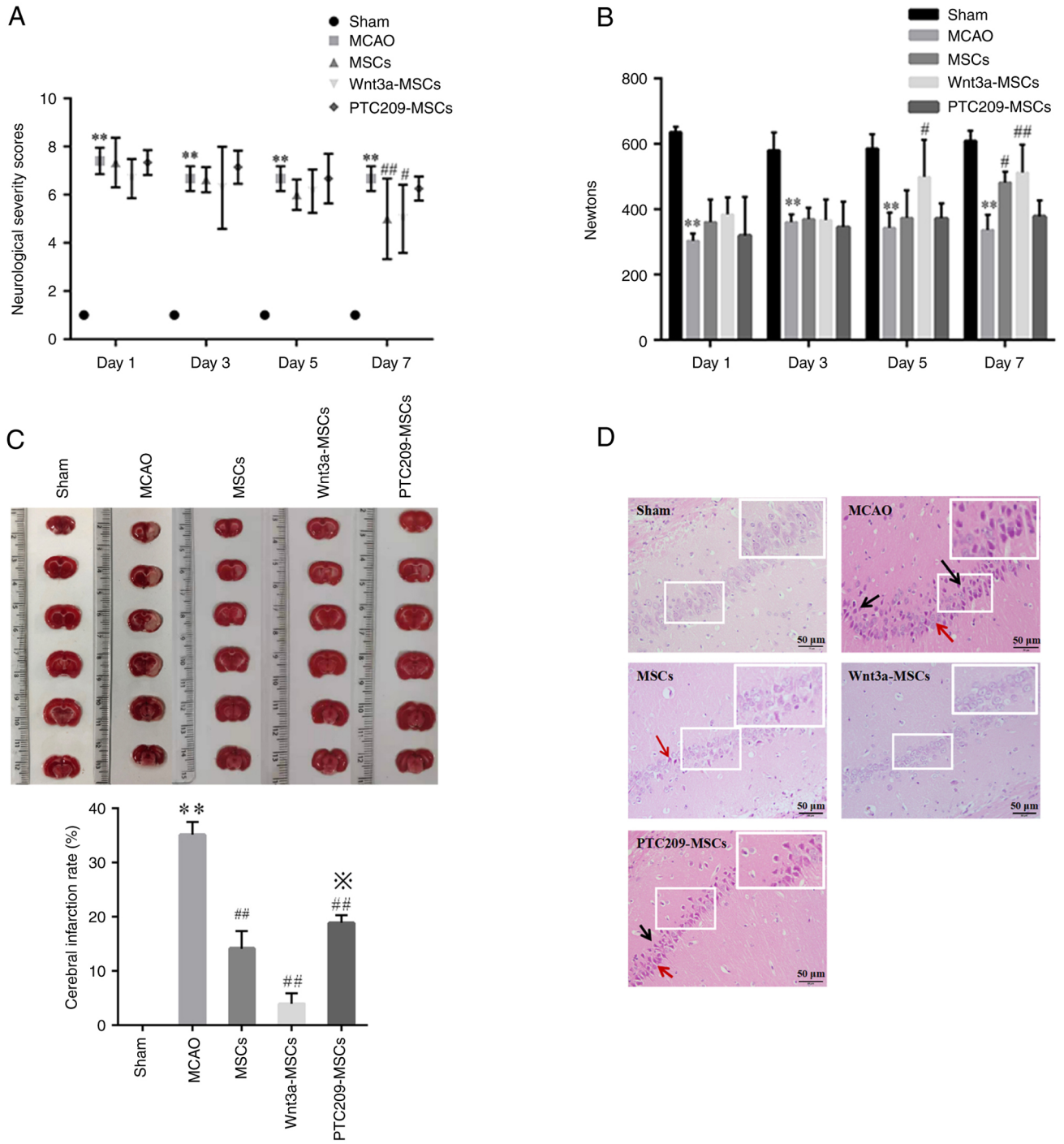

Figure 6. Role of B lymphoma Mo-MLV insertion region 1 homolog in MSC transplantation to repair pathological injury in a rat model of MCAO. (A) Neurological Severity Score results. (B) Grip measurement results. **P<0.01 vs. Sham; $^{\#}$P<0.05 and $^{\#\#}$P<0.01 vs. MCAO. (C) Triphenyltetrazolium chloride staining results for each group. **P<0.01 vs. Sham; $^{\#\#}$P<0.01 vs. MCAO, $^{\square}$P<0.05 vs. MSCs. (D) Pathological staining of the CA1 area in the hippocampal region of rat brain tissue in each group. Black arrows indicate degenerated and atrophied neuronal cells, and red arrows indicate tissue interstitial spaces. MCAO, middle cerebral artery occlusion; MSCs, mesenchymal stem cells.

an improvement in grasp strength on days 5 and 7, whereas the PTC209-MSCs group did not show any significant improvement at all time points. The TTC staining results indicated uniformly symmetric brain tissue coloring without infarction in the Sham group rats, whereas different degrees of infarction conditions were observed in the brain tissues of the MCAO group and the three MSC transplantation groups (Fig. 6C). The infarction rate in brain tissue was significantly decreased in all three groups receiving MSC transplantation compared with that in the MCAO group. Moreover, the Wnt3a-MSCs group had a lower infarction rate than the MSCs group, whereas the PTC209-MSCs group had an increased infarction rate compared with that in the MSCs group. After performing H&E staining on brain tissue sections, a normal and clear cell structure was observed in the Sham group; by contrast, the MCAO group exhibited more deeply stained, degenerated and atrophied neuronal cells, as well as a markedly enlarged tissue gap (Fig. 6D). The three groups that underwent MSC

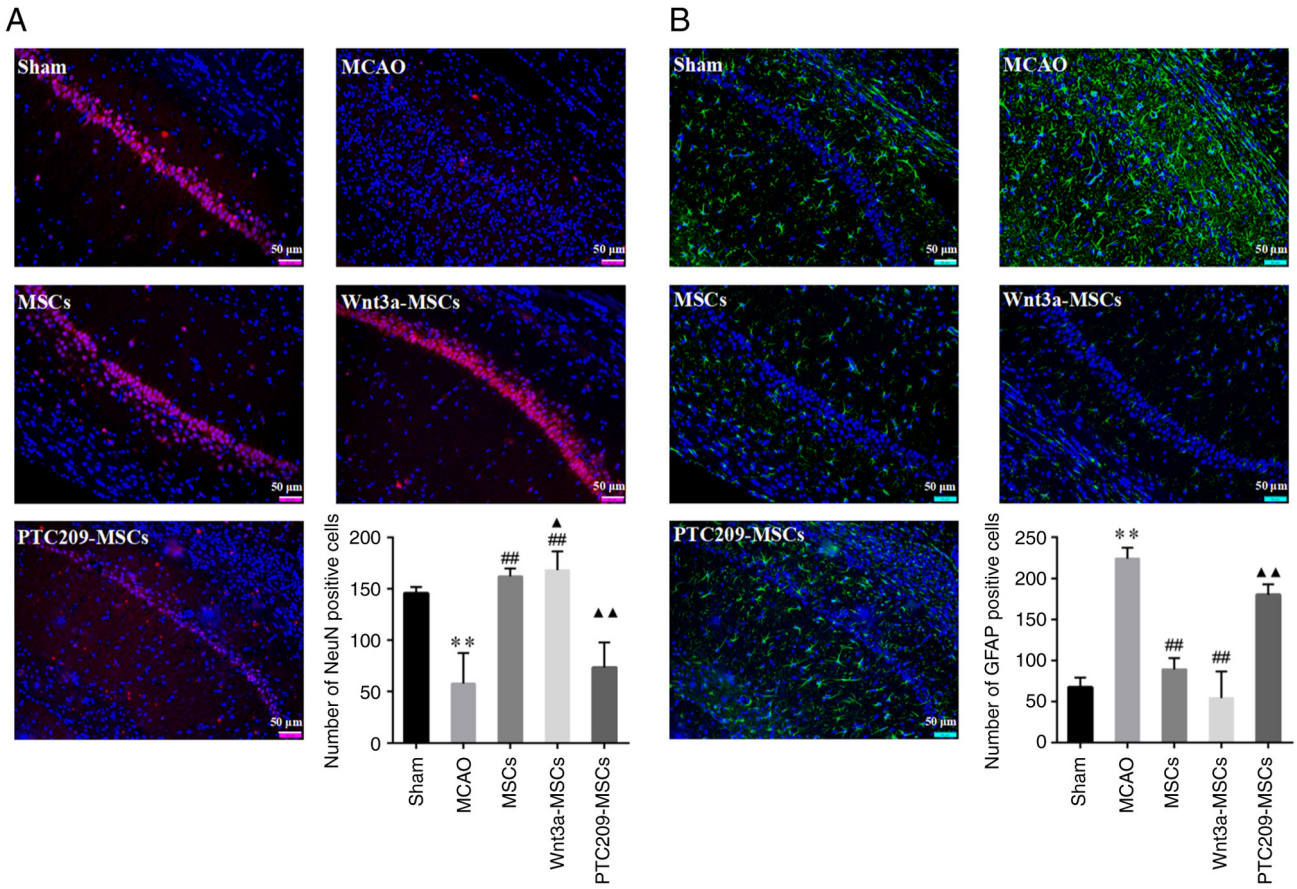

Figure 7. Effects of downregulation of B lymphoma Mo-MLV insertion region 1 homolog on neurological recovery in rats. Number of (A) NeuN-positive cells and (B) GFAP-positive cells in the CA1 region of the hippocampus in each group of rats. **P<0.01 vs. Sham; $^{\#\#}$P<0.01 vs. MCAO; $^{\blacktriangle}$P<0.05, $^{\blacktriangle\blacktriangle}$P<0.01 vs. MSCs. GFAP, glial fibrillary acidic protein; MCAO, middle cerebral artery occlusion; MSCs, mesenchymal stem cells.

transplantation exhibited fewer cellular wrinkles and necrotic areas compared with the MCAO group, with varying degrees of improvement in tissue damage. However, among these three groups, there were still more wrinkled and deeply stained cells in the PTC209-MSCs group. This suggests that Wnt3a may enhance the neural repair function of MSCs and PTC209 could attenuate the neural repair function of MSCs.

All of the aforementioned findings indicated that the MCAO model rats developed notable behavioral disturbances following ischemic brain damage, whereas neurological function and localized brain infarction symptoms improved following transplantation of MSCs into MCAO model rats. Treatment of MSCs with Wnt3a further improved infarction symptoms in damaged brain tissues, whereas downregulation of Bmi1 using PTC209 hindered the reduction of the cerebral infarction rate, thus suggesting that Bmi1 serves a role in repairing IBI through MSC transplantation.

Downregulation of Bmi1 inhibits recovery of neurological function in MCAO rats. Sections of the rat hippocampal CA1 area were stained with red fluorescence for NeuN-positive cells and green fluorescence for GFAP-positive cells. The NeuN immunofluorescence results indicated a significant decrease in the number of NeuN-positive cells in the MCAO group as compared with in the Sham group (Fig. 7A). By contrast, the MSCs and Wnt3a-MSCs groups exhibited a significant increase in NeuN-positive cells compared with those in the MCAO group, whereas the PTC209-MSCs group showed no significant difference. When compared with the MSCs group, the Wnt3a-MSCs group showed a significant increase in NeuN staining while the PTC209-MSCs group showed a significant decrease. By contrast, the GFAP immunofluorescence results revealed a notable increase in GFAP-positive cells in the MCAO group when compared with the Sham group (Fig. 7B). Furthermore, the MSCs and Wnt3a-MSCs groups exhibited a significant reduction in the number of GFAP-positive cells compared with in the MCAO group, whereas there was no statistically significant difference in GFAP staining between the PTC209-MSCs group and the MCAO group. The number of GFAP-positive cells was significantly increased in the PTC209-MSCs group compared with the MSCs group.

The results of western blotting indicated that in the MCAO group, NeuN protein expression was lower and GFAP expression was higher compared with that in the Sham group (Fig. 8). Conversely, in the MSCs and Wnt3a-MSCs groups, NeuN protein expression was higher whereas GFAP protein expression was lower than that in the MCAO group. Notably, neither NeuN or GFAP expression was significantly altered in the Wnt3a-MSCs group compared with in the MSCs group. NeuN expression was decreased and GFAP expression was elevated in the PTC209-MSCs group compared with the MSCs group.

The present findings suggested that Wnt3a may promote an increase in the number of neurons in the CA1 region of the rat hippocampus and enhance the neural repair function of MSCs,

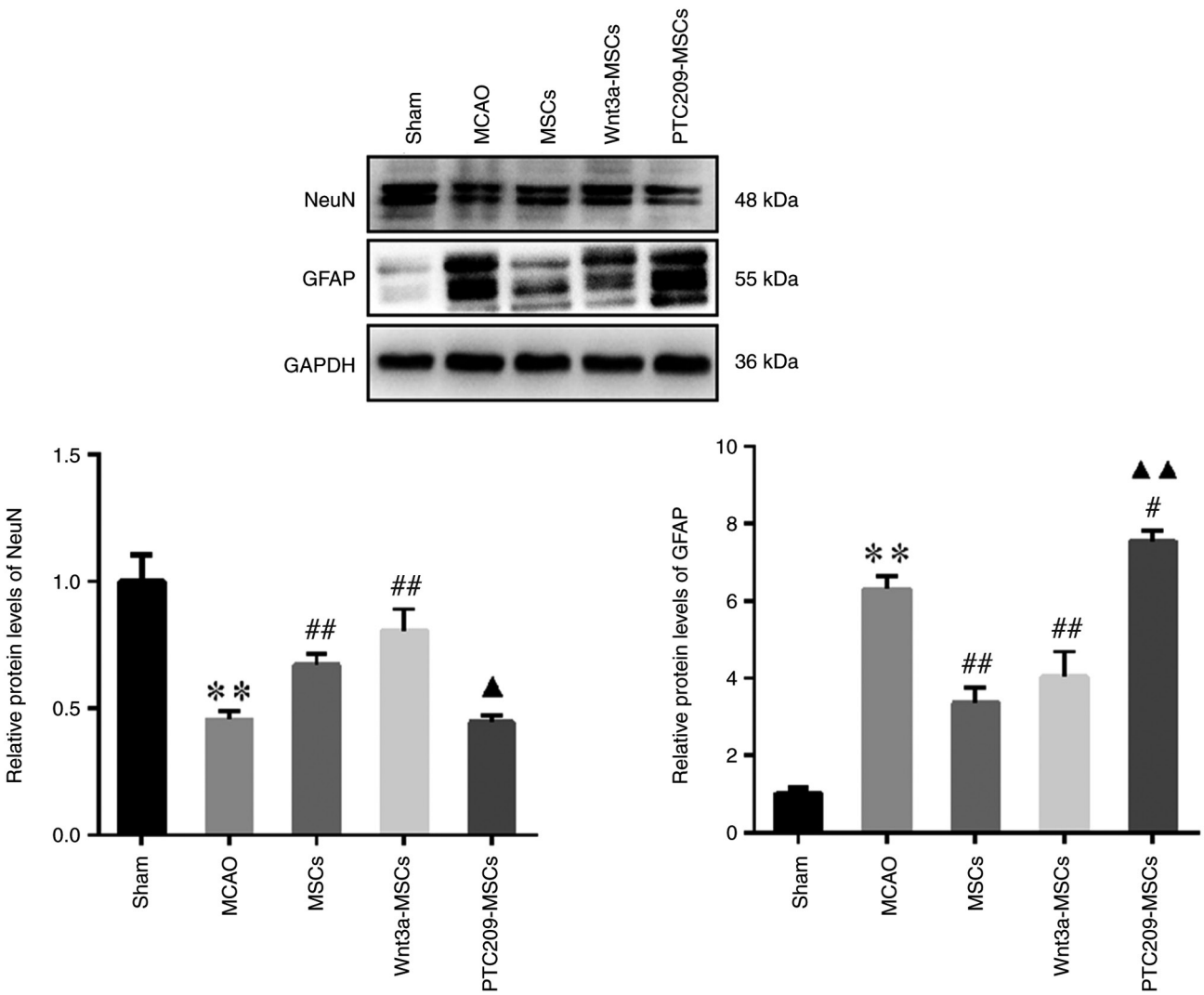

Figure 8. NeuN and GFAP protein expression in each group. For GFAP and NeuN, all visible bands were included in the semi-quantitative analysis. **P<0.01 vs. Sham; ##P<0.01 vs. MCAO; ▲P<0.05, ▲▲P<0.01 vs. MSCs. GFAP, glial fibrillary acidic protein; MCAO, middle cerebral artery occlusion; MSCs, mesenchymal stem cells.

whereas downregulation of Bmi1 could inhibit the increased neuronal number and the decrease of astrocyte number in the CA1 region of the hippocampus of MSC-transplanted rats, and may thus suppress neural repair.

Discussion

IBIs are associated with high morbidity, disability and mortality due to their complex pathogenesis, with MCAO being a prevalent cause. Cerebral ischemia results in restored blood supply after a certain period of time; however, brain function is not restored and is accompanied by severe delayed neuronal apoptosis and necrosis, leading to brain dysfunction. Notably, stem cell therapy utilizing MSCs has become a promising approach for treating neurological disorders (29). However, the altered homeostasis of the internal brain tissue environment in IBI adversely affects the survival, proliferation and effective differentiation rate of transplanted stem cells; these factors notably impede the efficacy of MSC transplantation (30,31). To address this issue, the present study showed that Wnt3a can promote MSC neural differentiation by upregulating the Wnt3a-RhoA signaling pathway. Investigations have shown that Wnt3a treatment or Wnt3a overexpression in MSCs activates both classical and non-classical Wnt signaling pathways (32). Several cytokines and chemokines, such as stromal cell-derived factor-1α, a CXC-type chemokine produced by bone marrow stromal cells, can induce the chemotactic migration of MSCs toward the injured part of the nerve and contribute to the repair of structure and function at the site of injury (33). In our previous study, it was found that upregulation of the Wnt3a-RhoA signaling pathway using Wnt3a could promote the migration of MSCs *in vitro* (27). Therefore, 10 ng/ml Wnt3a was used in the present study.

MSCs have the potential to differentiate into neural cells, offering a promising option for treating IBI. The present study confirmed that BME induced the differentiation of MSCs to the neuronal lineage, as indicated by positive staining of Nestin, a marker for tumor stem cells, NSCs and astrocytes and GFAP, an astrocyte surface marker.

Cerebral ischemia instigates neuronal necrosis, apoptosis and progressive neuronal depletion, particularly in the CA1 section of the hippocampus, culminating in notable debilitation

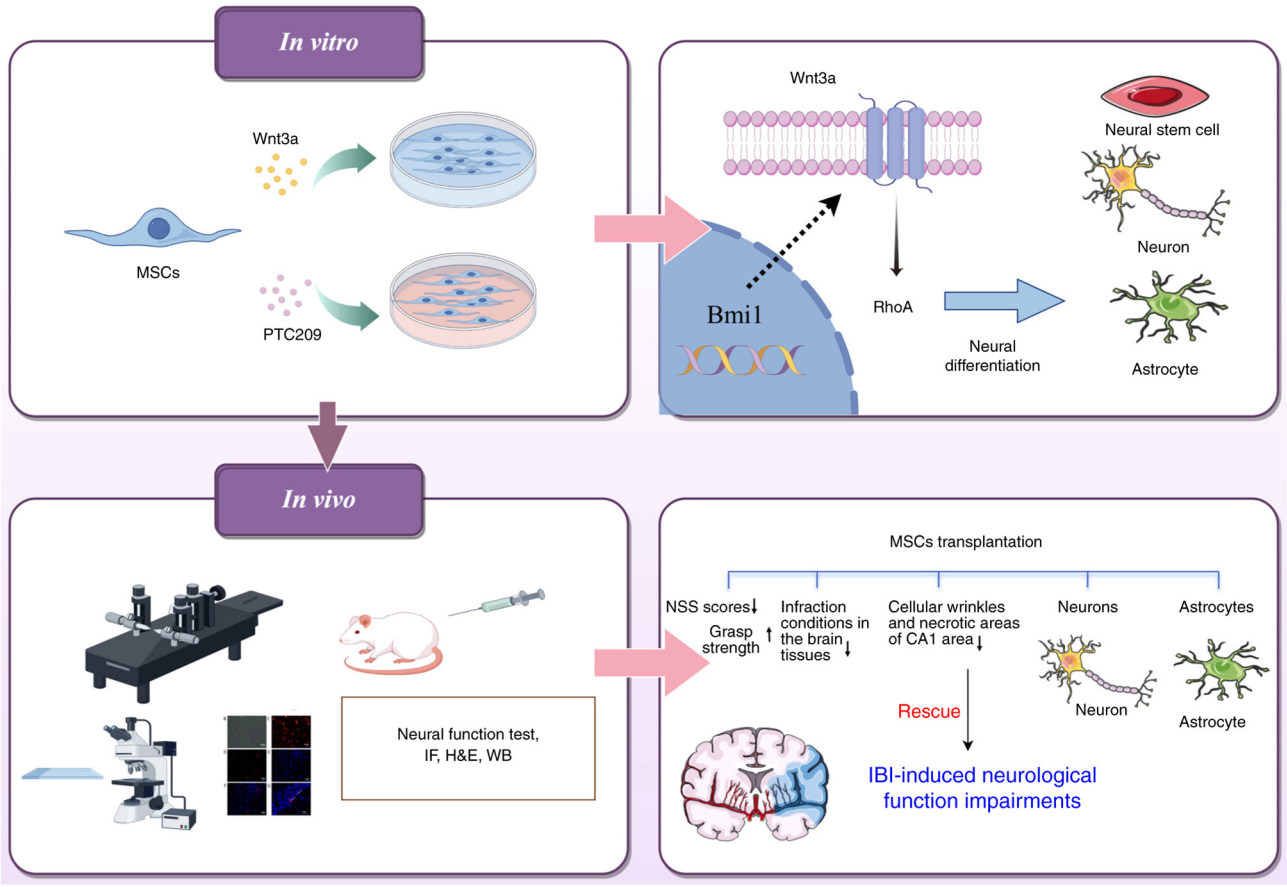

Figure 9. The mechanism underlying the effects of Bmi1 on MSC transplantation-induced ischemic brain injury repair. *In vitro* experiments used Wnt3a and PTC209 to treat MSCs to explore the roles and regulatory mechanisms of the Bmi1 and Wnt3a-Rhoa signaling pathways in the neural differentiation of MSCs. *In vivo* experiments were conducted to investigate the role of the Bmi1 and Wnt3a-RhoA signaling pathway in brain injury repair in MCAO rats and its mechanism. Different MSCs were transplanted into rat brain tissues after *in vitro* labeling, after which, the ischemic brain injury in each group was compared and the recovery of neurological function was assessed. Bmi1, B lymphoma Mo-MLV insertion region 1 homolog; H&E, hematoxylin and eosin; IF, immunofluorescence; MSCs, mesenchymal stem cells; NSS, Neurological Severity Score; WB, western blotting.

in cognitive ability, spatial perception and behavior (34). The CA1 region of the hippocampus in the brain is particularly vulnerable to IBI, and the neuronal cells within this area are susceptible to necrosis and apoptosis following such an injury (35). This region of the hippocampus is comprised of dense, large neurons, and these vertebral neurons are the principal output neurons of the hippocampus (36), which have the capacity to selectively transmit different behavioral information to various target areas (37). Consequently, the CA1 region of the hippocampus was selected as the primary assessment target in the present study. In the present study, rats that underwent MCAO showed notable behavioral deficits after IBI episodes. CM-Dil-labeled cells were visible in the hippocampal region of rat brain tissue sections after MSCs transplantation, and the NSS and grasping ability of rats gradually improved. Transplanting MSCs promoted neurogenesis, which aligns with the results indicating that MSCs have the ability to nourish cells, promote cell proliferation and differentiation, inhibit cell death and regulate homeostasis in the injured area (38-41). The current study indicated that upregulation of the Wnt3a-RhoA signaling pathway in MSCs led to an increase in the number of neurons in the CA1 region of the rat hippocampus by immunofluorescence staining and H&E staining, thus improving the neural repair ability of MSCs.

The Bmi1 protein belongs to the multi-comb inhibitory complex 1 family, and contributes to various biological processes, including embryonic development, organogenesis, tumorigenesis, and stem cell stabilization and differentiation (42). The results of the current study demonstrated an increase in Bmi1 protein expression during the induction of neural differentiation of MSCs *in vitro*, suggesting its potential involvement in this process. However, the effects of Bmi1 on the neural differentiation of MSCs and the underlying mechanism remain unclear. Notably, Bmi1 acts as an oncogene, and its anomalous expression is associated with the progression and drug resistance of various types of cancer, including bladder cancer and B-cell lymphoma (43,44). Therefore, the present study implemented targeted small molecule inhibition of Bmi1 to specifically restrict Bmi1 levels, enabling the investigation of its association with and function in stem cell self-renewal and differentiation. The Bmi1-selective inhibitor PTC209 was initially screened by Kreso *et al* (45) through small-molecule gene expression modulation technology. As demonstrated in a preceding study, a concentration of 1 μM of the small molecule compound PTC-209 was shown to inhibit the expression of Bmi1 during the process of induced pluripotent stem cell differentiation (46). The findings of the present study demonstrated that 1 μmol/l PTC209 exerted no effect

on the proliferation of MSCs. Furthermore, the inhibition of Bmi1 expression by PTC209 impeded the differentiation of MSCs towards astrocytes and neurons during BME-induced neural differentiation of MSCs *in vitro*.

NeuN is a neuronal protein the expression of which directly reflects the maturity of neurons, whereas GFAP acts as a marker for astrocyte activation. GFAP upregulation leads to a low percentage of NeuN protein phosphorylation and the formation of glial scarring, which hinders axon regeneration and thus negatively affects the repair of neural tissue structures. Changes in the expression of these two proteins may indicate the extent of nerve cell injury caused by cerebral ischemia (47). In the current study, the quantity of neurons and astrocytes were analyzed in brain tissues following MSC transplantation. The outcomes revealed that downregulation of Bmi1 by PTC209 inhibited the increase in neuron number and the decrease in astrocytes in the CA1 region of the hippocampus of MSC-transplanted rats and attenuated the frontal neural repair ability of MSCs. It may be hypothesized that the upregulation of GFAP resulting from reduced Bmi1 expression following IBI in rats may hinder CA1 hippocampal neuron repair and compromise the neural repair capacity of MSCs. It is important to note that the experimental results differed slightly due to the different experimental conditions employed in the present study between *in vitro* and *in vivo* experiments. For example, the results of *in vitro* experiments demonstrated that after inducing neural differentiation of MSCs, GFAP-positive cells could be observed under a microscope in the BME and Wnt3a groups, whereas GFAP-positive cells were almost unobservable in the PTC209 group. Conversely, the *in vivo* experiments demonstrated that the MCAO group exhibited significantly higher levels of GFAP-positive cells compared with the Sham group, whereas the MSCs and Wnt3a-MSCs groups exhibited a decrease in GFAP-positive cells compared with the MCAO group. A comprehensive review of the literature on GFAP revealed its expression in the intermediate filaments of the astrocyte lineage, thus serving as a marker for astrocytes. Astrocytes can form physical barriers to isolate damaged tissues, regulate blood flow after ischemia, promote the blood-brain barrier, support myelin formation and provide mechanical strength; however, it is important to note that prolonged upregulation of GFAP and proliferation of astrocytes can result in neurological damage, as well as the inhibition of the proliferation of mature brain neurons and protrusion extension (48-50). It is possible that the results of the *in vitro* and *in vivo* experiments are not completely uniform because of the different time and conditions for inducing neural differentiation *in vitro* and nerve injury *in vivo*.

Numerous studies have demonstrated that Bmi1 can regulate Wnt signaling in various types of cells (51-54). To further explore the relationship between Bmi1 and the Wnt3a-RhoA signaling pathway, the present study examined the effects of Wnt3a-induced upregulation of the Wnt3a-RhoA signaling pathway and PTC209-induced inhibition of Bmi1 on the expression of proteins related to Bmi1 and the Wnt3a-RhoA signaling pathway. No significant difference in Bmi1 protein expression was observed after upregulating Wnt3a-RhoA in MSCs; however, downregulation of Bmi1 in MSCs resulted in a significant decrease in the protein expression levels of both Wnt3a and RhoA. These findings suggested that Bmi1 might serve a role in the neural differentiation process of MSCs by regulating the expression of Wnt3a and RhoA.

In summary, the repair of IBI by MSC transplantation is a multifaceted process that is affected by numerous factors. The utilization of MSCs in the replacement of damaged or functionally deficient neural tissue for the treatment of IBI represents a highly promising therapeutic modality. It has been reported that Bmi1 is essential for the maintenance of stemness in a variety of stem cells (55,56); however, studies on Bmi1 in MSCs are still scarce. The present study aimed to explore the mechanism of Bmi1 and the Wnt3a-RhoA signaling pathway on the *in vitro* neural differentiation of MSCs and on *in vivo* IBI repair. Through the findings of the *in vivo* and *in vitro* experiments, it was indicated that Bmi1 may regulate neural differentiation of MSCs through the Wnt3a-RhoA signaling pathway to repair ischemic brain injury in rats (Fig. 9). In the current study, the role of Bmi1 in the repair of IBI by MSC transplantation was investigated. With the continuous development of translational and neuroregenerative medicine, these findings may provide novel insights and targets for the treatment of IBI. Furthermore, Bmi1 could serve as a new therapeutic target for the treatment of neurological diseases. Nevertheless, the present study is not without limitations. Firstly, only the Wnt3a and RhoA components of the Wnt signaling pathway were analyzed. Secondly, the antagonistic effect of Wnt3a, an agonist of Wnt3a-RhoA, on PTC209, a Bmi1 inhibitor, requires further investigation. It is evident that further exploration is required to gain a more comprehensive understanding of the subject; this necessitates the conduction of additional in-depth studies. Finally, following extensive consultation of the literature, normal MSC culture conditions were employed in the *in vitro* experiments to explore the mechanism. The paucity of studies based on ischemic cell conditions was noted and it was acknowledged that this area should be a focus of future research.

In conclusion, the results of the present study provide conclusive evidence that suggests Bmi1 may serve a crucial role in the process of neural differentiation of MSCs by regulating the expression of Wnt3a and RhoA. Furthermore, the findings indicated that elevating the Wnt3a-RhoA signaling pathway in MSCs may foster the restoration of neural function in rats with brain injuries. Conversely, downregulation of Bmi1 in MSCs may impede the recovery of neural function in brain-damaged rats.

Acknowledgements

Not applicable.

Funding

This work was supported by the Research Project of Zhejiang Chinese Medical University (grant no. 2022JKZKTS21) and the Research Project on Laboratory Work in Universities of Zhejiang Province (grant no.YB202268).

Availability of data and materials

The data generated in the present study may be requested from the corresponding author.

Authors' contributions

KC performed all relevant experiments and prepared the drafts. HZ performed the *in vitro* experiments. JZ and YZ performed the *in vivo* experiments. XD prepared the drafts, revised the manuscript, and analyzed and interpreted the data. QY and LZ designed and directed the project. All authors confirm the authenticity of all the raw data. All authors read and approved the final manuscript.

Ethics approval and consent to participate

All animal experiments were approved by the Animal Ethical and Welfare Committee of Zhejiang Chinese Medical University (approval no. 20210524-05; review no. IACUC-202108-05).

Patient consent for publication

Not applicable.

Competing interests

The authors declare that they have no competing interests.

References

1. Global burden of 369 diseases and injuries in 204 countries and territories, 1990-2019: A systematic analysis for the Global Burden of Disease Study 2019. Lancet 396: 1204-1222, 2020.
2. McIntyre CW and Goldsmith DJ: Ischemic brain injury in hemodialysis patients: Which is more dangerous, hypertension or intradialytic hypotension? Kidney Int 87: 1109-1115, 2015.
3. Liu X and Jia X: Neuroprotection of stem cells against ischemic brain injury: From bench to clinic. Transl Stroke Res 15: 691-713, 2024.
4. Sakai S and Shichita T: Inflammation and neural repair after ischemic brain injury. Neurochem Int 130: 104316, 2019.
5. Nie X, Leng X, Miao Z, Fisher M and Liu L: Clinically ineffective reperfusion after endovascular therapy in acute ischemic stroke. Stroke 54: 873-881, 2023.
6. Guo Y, Peng Y, Zeng H and Chen G: Progress in mesenchymal stem cell therapy for ischemic stroke. Stem Cells Int 2021: 9923566, 2021.
7. Chrostek MR, Fellows EG, Crane AT, Grande AW and Low WC: Efficacy of stem Cell-based therapies for stroke. Brain Res 1722: 146362, 2019.
8. Li C, Sun T and Jiang C: Recent advances in nanomedicines for the treatment of ischemic stroke. Acta Pharm Sin B 11: 1767-1788, 2021.
9. Leveque X, Hochane M, Geraldo F, Dumont S, Gratas C, Oliver L, Gaignier C, Trichet V, Layrolle P, Heymann D, *et al*: Low-dose pesticide mixture induces accelerated mesenchymal stem cell aging in vitro. Stem Cells 37: 1083-1094, 2019.
10. Cao Z, Xie Y, Yu L, Li Y and Wang Y: Hepatocyte growth factor (HGF) and stem cell factor (SCF) maintained the stemness of human bone marrow mesenchymal stem cells (hBMSCs) during long-term expansion by preserving mitochondrial function via the PI3K/AKT, ERK1/2, and STAT3 signaling pathways. Stem Cell Res Ther 11: 329, 2020.
11. Zhang L, Xiong N, Liu Y and Gan L: Biomimetic cell-adhesive ligand-functionalized peptide composite hydrogels maintain stemness of human amniotic mesenchymal stem cells. Regen Biomater 8: rbaa057, 2021.
12. Zhou T, Yang Y, Chen Q and Xie L: Glutamine metabolism is essential for stemness of bone marrow mesenchymal stem cells and bone homeostasis Stem Cells Int 2019: 8928934, 2019.
13. de Morree A and Rando TA: Regulation of adult stem cell quiescence and its functions in the maintenance of tissue integrity. Nat Rev Mol Cell Biol 24: 334-354, 2023.
14. Sahasrabuddhe AA: BMI1: A biomarker of hematologic malignancies. Biomark Cancer 8: 65-75, 2016.
15. Yang J, Xue J, Hu W, Zhang L, Xu R, Wu S, Wang J, Ma J, Wei J, Wang Y, *et al*: Human embryonic stem cell-derived mesenchymal stem cell secretome reverts silica-induced airway epithelial cell injury by regulating Bmi1 signaling. Environ Toxicol 38: 2084-2099, 2023.
16. Zheng X, Wang Q, Xie Z and Li J: The elevated level of IL-1α in the bone marrow of aged mice leads to MSC senescence partly by down-regulating Bmi-1. Exp Gerontol 148: 111313, 2021.
17. Mich JK, Signer RA, Nakada D, Pineda A, Burgess RJ, Vue TY, Johnson JE and Morrison SJ: Prospective identification of functionally distinct stem cells and neurosphere-initiating cells in adult mouse forebrain. Elife 3: e02669, 2014.
18. Kraus L, Bryan C, Wagner M, Kino T, Gunchenko M, Jalal W, Khan M and Mohsin S: Bmi1 augments proliferation and survival of cortical Bone-derived stem cells after injury through novel epigenetic signaling via histone 3 Regulation. Int J Mol Sci 22: 7813, 2021.
19. Zhang D, Huang J, Wang F, Ding H, Cui Y, Yang Y, Xu J, Luo H, Gao Y, Pan L, *et al*: BMI1 regulates multiple myeloma-associated macrophage's pro-myeloma functions. Cell Death Dis 12: 495, 2021.
20. Russell JO and Monga SP: Wnt/β-Catenin signaling in liver development, homeostasis, and pathobiology. Annu Rev Pathol 13: 351-378, 2018.
21. Yu Q, Liu L, Duan Y, Wang Y, Xuan X, Zhou L and Liu W: Wnt/β-catenin signaling regulates neuronal differentiation of mesenchymal stem cells. Biochem Biophys Res Commun 439: 297-302, 2013.
22. Schunk SJ, Floege J, Fliser D and Speer T: WNT-β-catenin signalling-a versatile player in kidney injury and repair, Nat Rev Nephrol 17: 172-184, 2021.
23. Torban E and Sokol SY: Planar cell polarity pathway in kidney development, function and disease. Nat Rev Nephrol 17: 369-385, 2021.
24. Bengoa-Vergniory N, Gorroño-Etxebarria I, González-Salazar I and Kypta RM: A switch from canonical to noncanonical Wnt signaling mediates early differentiation of human neural stem cells. Stem Cells 32: 3196-208, 2014.
25. Govek EE, Newey SE and Van Aelst L: The role of the Rho GTPases in neuronal development. Genes Dev 19: 1-49, 2005.
26. Zhou Y, Li HQ, Lu L, Fu DL, Liu AJ, Li JH and Zheng GQ: Ginsenoside Rg1 provides neuroprotection against blood brain barrier disruption and neurological injury in a rat model of cerebral ischemia/reperfusion through downregulation of aquaporin 4 expression. Phytomedicine 21: 998-1003, 2014.
27. Yao P, Yu Q, Zhu L, Li J, Zhou X, Wu L, Cai Y, Shen H and Zhou L: Wnt/PCP pathway regulates the migration and neural differentiation of mesenchymal stem cells in vitro. Folia Histochem Cytobiol 60: 44-54, 2022.
28. Zaghloul RA, Elsherbiny NM, Kenawy HI, El-Karef A, Eissa LA and El-Shishtawy MM: Hepatoprotective effect of hesperidin in hepatocellular carcinoma: Involvement of Wnt signaling pathways. Life Sci 185: 114-125, 2017.
29. Liu D, Ye Y, Xu L, Yuan W and Zhang Q: Icariin and mesenchymal stem cells synergistically promote angiogenesis and neurogenesis after cerebral ischemia via PI3K and ERK1/2 pathways. Biomed Pharmacother 108: 663-669, 2018.
30. Goldman SA: Stem and Progenitor Cell-based therapy of the central nervous system: Hopes, hype, and wishful thinking. Cell Stem Cell 18: 174-188, 2016.
31. Li Q, Guo Y, Chen F, Liu J and Jin P: Stromal cell-derived factor-1 promotes human adipose tissue-derived stem cell survival and chronic wound healing. Exp Ther Med 12: 45-50, 2016.
32. Meng Z, Feng G, Hu X, Yang L, Yang X and Jin Q: SDF Factor-1α promotes the migration, proliferation, and osteogenic differentiation of mouse bone marrow mesenchymal stem cells through the Wnt/β-catenin pathway. Stem Cells Dev 30: 106-117, 2021.
33. Marquez-Curtis LA and Janowska-Wieczorek A: Enhancing the migration ability of mesenchymal stromal cells by targeting the SDF-1/CXCR4 axis. Biomed Res Int 2013: 561098, 2013.
34. Liu P, Xu J, Chen Y, Xu Q, Zhang W, Hu B, Li A and Zhu Q: Electrophysiological signatures in global cerebral ischemia: Neuroprotection via chemogenetic inhibition of CA1 pyramidal neurons in rats. J Am Heart Assoc 13: e036146, 2024.
35. Fu HY, Cui Y, Li Q, Wang D, Li H, Yang L, Wang DJ and Zhou JW: LAMP-2A ablation in hippocampal CA1 astrocytes confers cerebroprotection and ameliorates neuronal injury after global brain ischemia. Brain Pathol 33: e13114, 2023.

36. Lalkovičová M, Bonová P, Burda J and Danielisová V: Effect of bradykinin postconditioning on ischemic and toxic brain damage. Neurochem Res 40: 1728-1738, 2015.
37. Mao M, Xu Y, Zhang XY, Yang L, An XB, Qu Y, Chai YN, Wang YR, Li TT and Ai J: MicroRNA-195 prevents hippocampal microglial/macrophage polarization towards the M1 phenotype induced by chronic brain hypoperfusion through regulating CX3CL1/CX3CR1 signaling. J Neuroinflammation 17: 244, 2020.
38. Chang CY, Liang MZ, Wu CC, Huang PY, Chen HI, Yet SF, Tsai JW, Kao CF and Chen L: WNT3A promotes neuronal regeneration upon traumatic brain injury. Int J Mol Sci 21: 1463, 2020.
39. He M, Shi X, Yang M, Yang T, Li T and Chen J: Mesenchymal stem cells-derived IL-6 activates AMPK/mTOR signaling to inhibit the proliferation of reactive astrocytes induced by hypoxic-ischemic brain damage. Exp Neurol 311: 15-32, 2019.
40. Pourheydar B, Soleimani Asl S, Azimzadeh M, Rezaei Moghadam A, Marzban A and Mehdizadeh M: Neuroprotective effects of bone marrow mesenchymal stem cells on bilateral common carotid arteries occlusion model of cerebral ischemia in rat. Behav Neurol 2016: 2964712, 2016.
41. Xin H, Katakowski M, Wang F, Qian JY, Liu XS, Ali MM, Buller B, Zhang ZG and Chopp M: MicroRNA cluster miR-17-92 cluster in exosomes enhance neuroplasticity and functional recovery after stroke in rats. Stroke 48: 747-753, 2017.
42. Park IK, Qian D, Kiel M, Becker MW, Pihalja M, Weissman IL, Morrison SJ and Clarke MF: Bmi-1 is required for maintenance of adult self-renewing haematopoietic stem cells. Nature 423: 635-642, 2003.
43. Wen T, Zhang X, Gao Y, Tian H, Fan L and Yang P: SOX4-BMI1 axis promotes non-small cell lung cancer progression and facilitates angiogenesis by suppressing ZNF24. Cell Death Dis 15: 698, 2024.
44. Zhao Y, Yang W, Zheng K, Chen J and Jin X: The role of BMI1 in endometrial cancer and other cancers. Gene 856: 147129, 2023.
45. Kreso A, van Galen P, Pedley NM, Lima-Fernandes E, Frelin C, Davis T, Cao L, Baiazitov R, Du W, Sydorenko N, *et al*: Self-renewal as a therapeutic target in human colorectal cancer. Nat Med 20: 29-36, 2014.
46. Shan W, Zhou L, Liu L, Lin D and Yu Q: Polycomb group protein Bmi1 is required for the neuronal differentiation of mouse induced pluripotent stem cells. Exp Ther Med 21: 619, 2021.
47. Okoh OS, Akintunde JK, Akamo AJ and Akpan U: Thymoquinone inhibits Neuroinflammatory mediators and vasoconstriction injury via NF-κB dependent NeuN/GFAP/Ki-67 in hypertensive Dams and F1 male pups on exposure to a mixture of Bisphenol-A analogues. Toxicol Appl Pharmacol 494: 117162, 2025.
48. Li M, Li Z, Yao Y, Jin WN, Wood K, Liu Q, Shi FD and Hao J: Astrocyte-derived interleukin-15 exacerbates ischemic brain injury via propagation of cellular immunity. Proc Natl Acad Sci USA 114: E396-E405, 2017.
49. Duan CL, Liu CW, Shen SW, Yu Z, Mo JL, Chen XH and Sun FY: Striatal astrocytes transdifferentiate into functional mature neurons following ischemic brain injury. Glia 63: 1660-1670, 2015.
50. Sullivan SM, Sullivan RK, Miller SM, Ireland Z, Björkman ST, Pow DV and Colditz PB: Phosphorylation of GFAP is associated with injury in the neonatal pig hypoxic-ischemic brain. Neurochem Res 282: 29414-29423, 2012.
51. Hosoya A, Takebe H, Seki-Kishimoto Y, Noguchi Y, Ninomiya T, Yukita A, Yoshiba N, Washio A, Iijima M, Morotomi T, *et al*: Polycomb protein Bmi1 promotes odontoblast differentiation by accelerating Wnt and BMP signaling pathways. Histochem Cell Biol 163: 11, 2024.
52. Yu J, Shen C, Lin M, Chen X, Dai X, Li Z, Wu Y, Fu Y, Lv J, Huang X, *et al*: BMI1 promotes spermatogonial stem cell maintenance by epigenetically repressing Wnt10b/β-catenin signaling. Int J Biol Sci 18: 2807-2820, 2022.
53. Chen MH, Fu LS, Zhang F, Yang Y and Wu XZ: LncAY controls BMI1 expression and activates BMI1/Wnt/β-catenin signaling axis in hepatocellular carcinoma. Life Sci 280: 119748, 2021.
54. Yu H, Gao R, Chen S, Liu X, Wang Q, Cai W, Vemula S, Fahey AC, Henley D, Kobayashi M, *et al*: Bmi1 regulates wnt signaling in hematopoietic stem and progenitor cells. Stem Cell Rev Rep 17: 2304-2313, 2021.
55. Bartucci M, Hussein MS, Huselid E, Flaherty K, Patrizii M, Laddha SV, Kui C, Bigos RA, Gilleran JA, El Ansary MMS, *et al*: Synthesis and characterization of novel BMI1 Inhibitors Targeting Cellular Self-renewal in hepatocellular carcinoma. Target Oncol 12: 449-462, 2017.
56. Zhu D, Wan X, Huang H, Chen X, Liang W, Zhao F, Lin T, Han J and Xie W: Knockdown of Bmi1 inhibits the stemness properties and tumorigenicity of human bladder cancer stem cell-like side population cells. Oncol Rep 31: 727-736, 2014.